JOURNAL OF GUIDANCE, CONTROL, AND DYNAMICS
Vol. 29, No. 5, September–October 2006

Certification and Design Issues for Rudder Control Systems in Transport Aircraft

Ronald A. Hess*
University of California, Davis, California 95616

DOI: 10.2514/1.18715

A recent transport aircraft accident involving inappropriate rudder inputs by the pilot flying has led to a series of National Transportation Safety Board recommendations regarding certification. In particular, certification standards are sought that will ensure safe handling qualities in the yaw axis throughout the flight envelope, including limits for rudder pedal sensitivity. This study is offered as a first step in establishing such standards. A review of current Code of Federal Regulations part 25 as regards rudder control is briefly summarized, as are pertinent sections of Federal Aviation Administration Advisory Circular 25-7A—Flight Test Guide for Certification of Transport Category Airplanes. An analytical investigation of possible piloting tasks for assessing rudder pedal force/feel systems is presented. The tasks reflect the philosophy of advisory circular 25-7A. A comparison of the pedal force/feel systems for three transport aircraft and four rotorcraft is presented. Three parameters for assessing the quality of pedal and rudder systems are discussed, a linearity index, maximum required pedal forces, and lateral acceleration at the pilot's station per unit of pedal force input above breakout.

Nomenclature

a_{ps}	=	lateral acceleration at the pilot's station, g's or ft/s^2
F_{BO}	=	pedal force/feel system breakout force, lbf
F_F	=	pedal force/feel system friction force, lbf
F_G	=	pedal force/feel system force gradient, lbf/ft or lbf/in
F_M	=	pedal force/feel system maximum force, lbf
K_{BW}	=	gain factor in virtual bobweight, ft–lbf/(rad/s^2)
$\dot{r}$	=	yaw acceleration, rad/s^2
Y_{FS}	=	transfer function of linear force/feel system
$Y_{p\psi}$	=	pilot model transfer function for heading loop
β	=	sideslip angle, rad
β_c	=	sideslip command, rad
δ_a	=	aileron angle, rad
δ_{ac}	=	command to aileron actuator, rad
δ_f	=	force applied to inceptor, lbf
δ_M	=	maximum pedal displacement, ft or in
δ_p	=	pedal input
δ_{PF}	=	force applied to pedal, lbf
δ_r	=	rudder angle, rad
δ_{rc}	=	command to rudder actuator, rad
δ_w	=	wheel input
ϕ	=	roll attitude, rad
ϕ_c	=	roll-attitude command, rad
ψ	=	heading, rad

I. Introduction

THE probable cause of the loss of American Airlines Flight 587 in November 2001 was established in [1]. Among the recommendations of this report were the following directed toward the Federal Aviation Administration (FAA):

1) Modify 14 Code of Federal Regulations Part 25 to include a certification standard that will ensure safe handling qualities in the yaw axis throughout the flight envelope, including limits for rudder pedal sensitivity . . . [A-04-56].

2) After the yaw axis certification standard recommended in Safety Recommendation A-04-56 has been established, review the designs of existing airplanes to determine if they meet the standard . . . [A-04-57].

The research to be described is an attempt to address the recommendations just outlined through a review of the current certification standards, a summary of a past study that may be pertinent to the certification issue, an analytical investigation of candidate piloting tasks that could be used in simulator evaluation of pedal force/feel systems, and a discussion of methods for assessing the quality of pedal and rudder control systems. The candidate tasks will reflect the philosophy of FAA advisory circular (AC) 25-7A [2]. The paper is organized as follows: Section II is a brief overview of current FAA certification standards as related to lateral-directional control and includes pertinent sections of AC 25-7A that address these standards. Attention will be focused upon FAA standards herein, for example, European Aviation Safety Agency (EASA) certification will not be discussed. Section III summarizes a previous study by the author related to rudder force/feel system design. Section IV presents a pilot/vehicle analysis and computer simulation of a particular transport aircraft rudder control system with an eye toward capturing the effect of pedal force/feel system nonlinearities on closed-loop pilot/vehicle performance. Section V presents force/feel system design considerations that may be pertinent to the certification process. Section VI is a comparison of some existing transport aircraft and rotorcraft force/feel systems. Section VII is a brief discussion of pertinent research results, and Sec. VIII presents major conclusions of the study.

II. Current Lateral-Directional Certification Standards and Advisory Circular 25-7A

Current Code of Federal Regulations Part 25 FAR regarding lateral/directional controllability and maneuverability, stability, flight maneuver, and gust conditions are contained in the following sections:

Section 25.143, subpart B a), b), c), and f). Flight: controllability and maneuverability

Section 25.147, subpart B a). Flight: controllability and maneuverability

Section 25.149, subpart B d). Flight: controllability and maneuverability

Section 25.171 subpart B. Flight: general

Section 25.177, subpart B c) and d). Flight: stability

Section 25.181, subpart B a). Flight: stability

Presented as Paper 6035 at the AIAA Atmospheric Flight Mechanics Conference and Exhibit, San Francisco, CA, 15–18 August 2005; received 9 July 2005; accepted for publication 3 January 2006.

*Professor, Department of Mechanical and Aeronautical Engineering. Associate Fellow AIAA

Section 25.351, subpart C a), b), c) and d). Structure: flight maneuver and gust conditions.

These FAR part 25 regulations associated with lateral/directional airplane characteristics deal only in very general terms with closed-loop pilot/vehicle behavior [3]. Requirements addressing such behavior are typically couched in broad terms such as "...must be controllable with normal use of the primary controls without requiring exceptional pilot skill" [25.147 subpart B a)]; or "Force, in pounds, applied to the...rudder pedals—for short term application 150 lbf ..." [25.143 subpart B c)]. The introduction of AC 25-7A in 1998 marked a departure from previous regulatory documents in that special attention was paid to closed-loop, pilot/vehicle behavior. Of course, like all AC material, these guidelines are not mandatory and do not constitute regulations. In addition, discussions of lateral-directional or yaw controllability are typically directed toward engine-out operation. Pertinent sections of AC 25-7A are discussed next. Attention will be focused on summarizing those sections of AC 25-7A that address a subset of the part 25 sections mentioned above, that is, 25.143, 147, and 181.

25.143 In addressing 25.143, AC 25-7A explicitly discusses aircraft pilot coupling (APC) or pilot-induced oscillation (PIO). In particular, it is stated:

> ... service experience has shown that compliance with only the quantitative, open-loop (pilot-out-of-the-loop) requirements does not guarantee that the required levels of flying qualities are achieved. Therefore, in order to ensure that the airplane has achieved the flying qualities required by sections 25.143a) and b), the airplane must be evaluated by test pilots conducting high-gain (wide-bandwidth) closed-loop tasks to determine that the potential of encountering adverse APC tendencies is minimal. For the most part, these tasks must be performed in actual flight. However, for conditions that are considered too dangerous to attempt in actual flight, the closed-loop evaluation tasks may be performed using a motion-base high-fidelity simulator if it can be validated for the flight conditions of interest.

AC 25-7A goes into considerable detail on procedures (flight test). The comments made are pertinent to all control inputs (axes) and are directed toward specific, closed-loop piloting tasks. Statements include the following:

> Evaluation of the actual task performance achieved ... is not recommended as a measure of proof of compliance. Only the pilot's rating of the APC characteristics is needed ....
>
> Tasks for a specific certification project should be based upon operational situations, flight testing maneuvers, or service difficulties that have produced APC events.
>
> Tasks described here may be useful in any given evaluation and have proven to be operationally significant in the past. It is not intended that these are the only tasks that may be used.... Other tasks may be developed and used as appropriate. For example, some manufacturers have used formation tracking tasks successfully in the investigation of these tendencies.[†]

AC 25-7A also goes into detail regarding assessing an aircraft's APC characteristics. This includes the description of specific maneuvers and tasks to be performed by evaluation pilots, that is, "capture" tasks and "fine tracking" tasks. The former are intended to evaluate handling qualities in gross acquisition tasks, while the latter imply tasks such as flying in a turbulent atmosphere. AC 25-7A describes APC rating criteria using a rating scale similar to that used in military handling qualities evaluations of APC characteristics.

25.147 In addressing directional control in 25-147, AC 25-7A suggests the following test procedure (task) with respect to directional control with inoperative engine(s):

> The airplane should be trimmed in level flight at the most critical altitude in accordance with section 25.21 c).[‡] Reasonably sudden changes in heading to the left and right using ailerons to maintain approximately wings-level flight should be made demonstrating a change of up to 15 deg or that at which 150 lb of rudder force is required. The airplane should be controllable and free from any hazardous characteristics during this maneuver.

25.181 AC 25-7A states that

> A typical test for lateral-directional dynamic stability is accomplished by a rudder doublet input at a rate and amplitude that will excite the lateral-directional response ("dutch roll"). The control input should be in phase with the airplane's oscillatory response.

Here, there is no mention of pilot closed-loop tracking. Rather, the rudder input is used strictly as a means to excite the dominant lateral/directional mode of the aircraft.

At the risk of oversimplification, one could state that current FAA certification standards regarding directional control may not be sufficient to identify potentially hazardous designs, particularly as concern force/feel system characteristics and their effect upon pilot high-gain closed-loop tracking in this axis. Advisory circular AC 25-7A calls attention to the importance of such high-gain piloting tasks in assessing vehicle handling qualities and possible APC susceptibility. Again, however, directional control tasks are only briefly discussed.

III. Summary of a Previous Study

An analytical study augmented by some limited desk-top simulation was summarized in Hess [6]. The major conclusions of [6] are summarized below.

1) A system survey of possible manual loop closure that could be employed by the pilot using rudder control led to an examination of two tracking strategies that could occur in large roll upsets and deliberate sideslip excursions. These strategies were a) combined use of aileron and rudder inputs and b) wings-level sideslip captures.

2) Using bandwidth/phase delay measures, the combined use of aileron and rudder inputs was predicted to result in low obtainable bandwidths in roll-attitude control. Although no bandwidth boundaries have been established for acceptable handling qualities in tasks involving combined use of aileron and rudder, the relatively small bandwidth values suggest poor handling qualities in such tasks in anything save low-bandwidth operations.

3) The pilot/vehicle analysis suggested that rudder force/feel systems with large sensitivities (or equivalently, low force gradients) could precipitate pilot-induced oscillations when combined use of ailerons and rudder was employed. This susceptibility could be attributed to large lateral accelerations occurring at the pilot's station.

4) The pilot/vehicle analysis suggested that wings-level sideslip captures might serve as a useful pilot-in-the-loop flight simulation task to investigate handling qualities issues involving rudder control.

5) The handling qualities and flight safety implications of high-gain, closed-loop tracking using combined aileron and rudder inputs that were suggested in the analysis were reflected in the desktop simulation.

6) A linearity index was defined to quantify the amount of nonlinearity (breakout, friction, etc.) in the quasistatic force/displacement characteristics of the pedal force/feel system. In a simplified pilot/vehicle analysis it was shown that small values of this index can lead to unpredictable and unsatisfactory response characteristics in closed-loop control.

IV. Pilot/Vehicle Analysis and Computer Simulation

A. Vehicle, Tasks, and Pilot Models

The following example follows closely that discussed in [6,7]. However, in the computer simulation of the pilot/vehicle system in these previous studies, the nonlinear force/feel characteristics did not include the hysteresis effect that may be caused by friction. This limitation is removed in the current treatment. The aircraft chosen for study is the DC-8 vehicle with stability derivatives defined for flight condition "8002" in McRuer et al. [8]. This flight

[†]Such tasks used by Boeing and Airbus are described in [4,5].

[‡]This article states "The controllability, stability, trim, and stalling characteristics of the airplane must be shown for each altitude up to the maximum expected in operation."

condition corresponds to an airspeed of 468.2 ft/s and an altitude of 15,000 ft. A yaw damper has been added to the basic airframe that increases the damping of the dutch roll mode from 0.11 to 0.4. Second-order actuator models have been included with transfer functions given by

$$\frac{\delta_r}{\delta_{r_c}} = \frac{\delta_a}{\delta_{a_c}} = \frac{20^2}{[s^2 + 2(0.707)20s + 20^2]} \text{ rad/rad} \quad (1)$$

Actuator rate and amplitude limits have also been included as follows: Aileron actuator amplitude and rate limits are set to ±20 deg and ±45 deg/s, respectively; rudder actuator amplitude and rate limits are set to ±15 deg and ±60 deg/s, respectively. The tasks chosen for study are the wings-level sideslip capture mentioned in Sec. III and a heading-hold sideslip capture task to be described.

Figure 1 is a block diagram representation of the hypothesized pilot/vehicle feedback structure for both tasks. Structural models of the human pilot are used in both the roll-attitude and sideslip loops. The structural model parameters are chosen as discussed in [6,7]. Nominal crossover frequencies of 2 rad/s are chosen initially for each loop, clearly indicating that the models meet the dictates of the crossover model of the human pilot [9]. Figure 2 shows the Bode plots for the resulting open-loop pilot/vehicle transfer functions.

B. Pedal Force/Feel Systems

Test pilots often refer to handling qualities "cliffs" as a metaphor to convey a sense of unexpected, dramatic, and excessively large aircraft responses to control inputs. Such cliffs are usually encountered when there are significant nonlinearities in the pilot/vehicle system. The most common of these nonlinearities are rate and amplitude limits in surface actuators and design features such as preloads, thresholds, and detents in cockpit inceptors [10]. Figure 3 compares the static, nonlinear, force-displacement characteristics of two pedal force/feel systems to be studied. These characteristics have not been chosen arbitrarily. They represent systems exhibiting large and small values of a "linearity index" introduced in [6,7]. This index is defined using Fig. 4. The figure shows the first quadrant of the quasistatic, force/displacement characteristics for a pedal force/feel system. The pedal breakout force (DA) and the friction force (BC) define the hysteresis for the system. For simplicity, these forces have been assumed to be equal in Fig. 4. This limitation will be removed in Sec. V. The slope of lines either lines AB or DC define the force gradient. The linearity index (LI) can be defined numerically as

$$\text{LI} = 1 - \frac{\text{Area(DABD)} + \text{Area(DBCD)}}{\text{Area}A\text{(DEBFD)}} \quad (2)$$

Applying Eq. (2) to systems A and B of Fig. 3 yields LI values of 0.35 and 0.84, respectively.

In addition to the static nonlinearity exhibited in Fig. 3, dynamic force/feel characteristics were included in both the wheel and pedal system through the inclusion of dynamics of the form

$$Y_{\text{FS}} = \frac{20^2}{[s^2 + 2(0.3)20s + 20^2]} \quad (3)$$

A comparison of the static and dynamic characteristics of the force/feel systems A and B in Fig. 3 is made in Figs. 5 and 6. Here, two sinusoidal force inputs identified as "fast" and "slow" are applied to each system. The slow and fast inputs have frequencies of 0.1 rad/s and 3 rad/s, respectively. As the figures indicate, both systems have significantly different force/displacement characteristics with the different input frequencies. The difference, of course, is attributable to the linear dynamics of linear force/feel system identified in Eq. (3).

In [6,7] a model-based description of how a pilot might cope with significant inceptor nonlinearities was presented. This approach employed a gain increment in the forward portion of the proprioceptive loop of the pilot model approximating the inverse of a

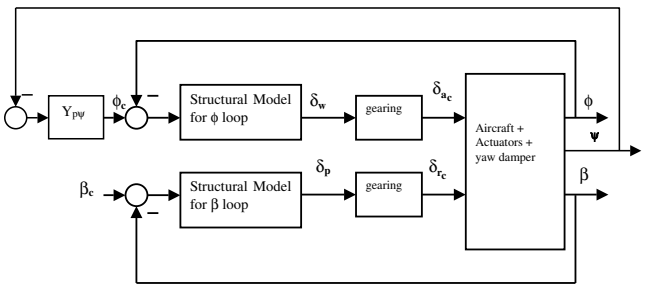

Fig. 1 Pilot/vehicle system for wings-level and heading-hold sideslip-capture tasks; for wings-level task, $Y_{p\psi} = 0$.

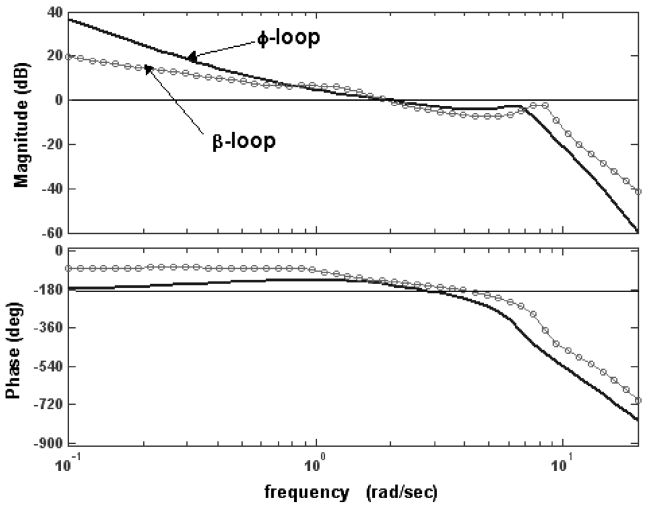

Fig. 2 Bode plots of open-loop pilot/vehicle transfer functions for ϕ and β loops in Fig. 1.

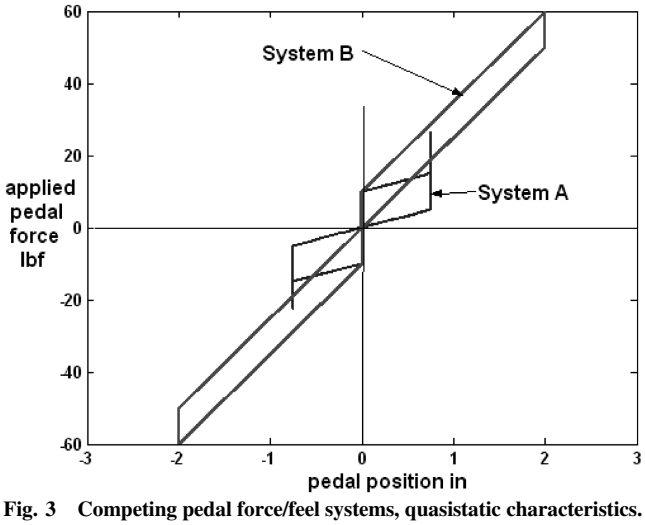

Fig. 3 Competing pedal force/feel systems, quasistatic characteristics.

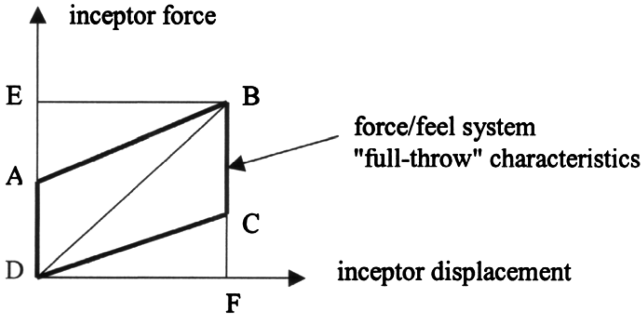

Fig. 4 Defining a "linearity index."

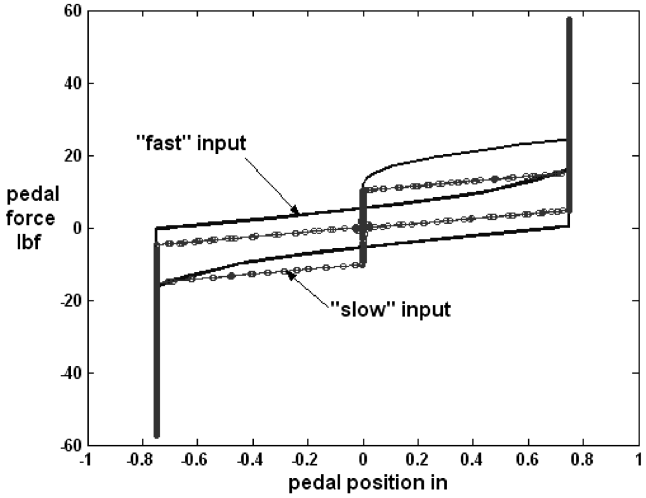

Fig. 5 Dynamic characteristics of force/feel system A with sinusoidal inputs of different frequencies.

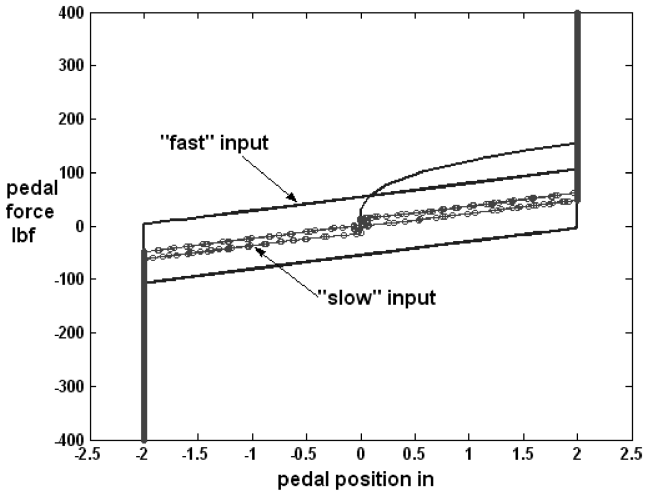

Fig. 6 Dynamic characteristics of force/feel system B with sinusoidal inputs of different frequency.

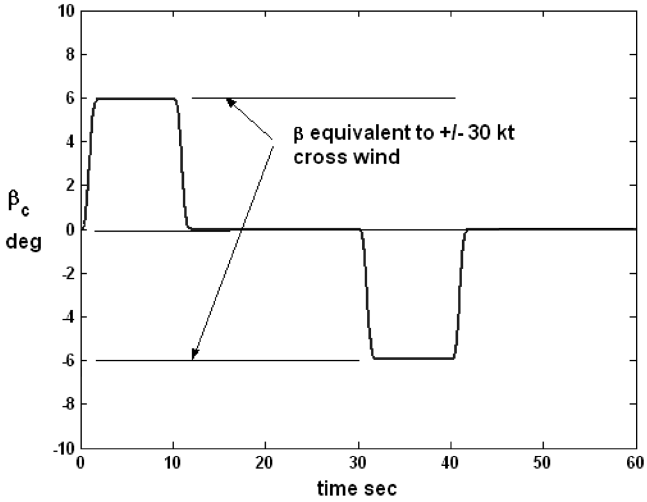

Fig. 7 Equivalent β command for wings-level sideslip capture task.

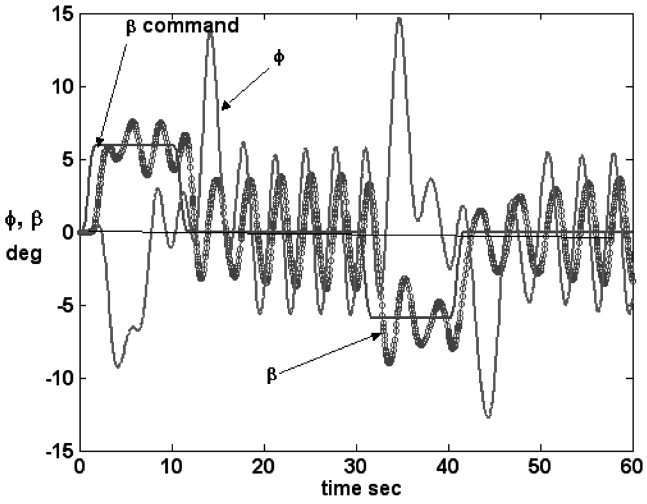

Fig. 8 Tracking performance using pedal force/feel system A from Fig. 3 in wings-level sideslip capture task.

Gaussian input describing function for a threshold nonlinearity. Hysteresis was not included in the computer simulations that used the structural pilot model. Because the force/feel dynamics employed in this study involve hysteresis, and not simply a threshold, the inverse threshold describing function approximation cannot be employed. Thus, no gain increments are employed in the pilot model in this study.

C. Wings-Level Sideslip-Capture Task and Computer Simulation

This task is described as follows: The pilot is to complete two alternating sideslip captures while attempting to maintain wings level. The magnitudes of the "commanded" sideslip angles are equivalent to a ± 30 kt steady cross wind being alternately introduced. The resulting commanded sideslip is shown in Fig. 7. Table 1 gives the performance requirements for the task. At this juncture, the requirements have been chosen simply for the purposes of exposition with no delineation of "desired" and "adequate" called out. The relatively large excursions in roll attitude allowed, even for desired performance, indicates that the "wings-level" description is somewhat optimistic for this task.

Table 1 Performance requirements for wings-level sideslip-capture task

Sideslip β	Roll attitude ϕ	Pedal inputs
Maximum steady-state error less than 0.5 deg No sustained oscillations greater than 1 deg	Maximum roll-attitude excursion 15 deg No sustained oscillations greater than 5 deg	No "stop-to-stop" reversals

Figures 8 and 9 show the model-derived pilot/vehicle performance for the two pedal force/feel systems of Fig. 3 for the wings-level sideslip-capture task. For this task, crossover frequencies for roll and sideslip loops were 1 rad/s and 2 rad/s, respectively. The larger crossover frequency for sideslip loop was chosen to represent aggressive pedal activity by the pilot. Figures 10 and 11 show the pedal position and rudder rate time histories for the two force/feel systems. Note the continuous "stop-to-stop" pedal inputs for system A and the frequent rudder actuator rate limiting for this system. The responses indicate that system A from Fig. 3 does not meet the performance requirements of Table 1 (Fig. 8 shows system A violating the sideslip performance requirements in addition to the stop-to-stop pedal inputs). By comparison, system B does meet the requirements. The lag apparent in Fig. 10 for system A as compared with system B is directly attributable to the existence of the larger hysteresis nonlinearity in the former as opposed to the latter force/feel system. Figure 12 shows the lateral acceleration at the pilot's station a_{ps}. Figure 13 shows pedal position vs pedal force trajectories. The linearity index defined in Eq. (2) and Fig. 4 appears to be a sensitive indicator of the overall acceptability of force/feel system characteristics. That is, the system with LI $= 0.35$ (system A) yields considerably poorer performance that the system with LI $=$ 0.84 (system B).

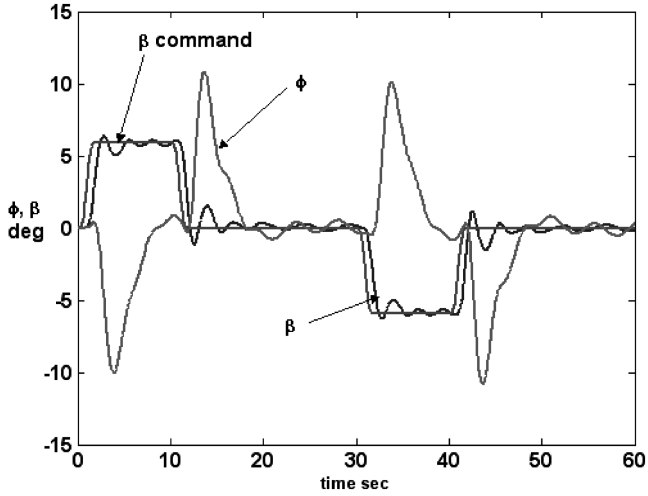

Fig. 9 Tracking performance using pedal force/feel system B from Fig. 3 in wings-level sideslip capture task.

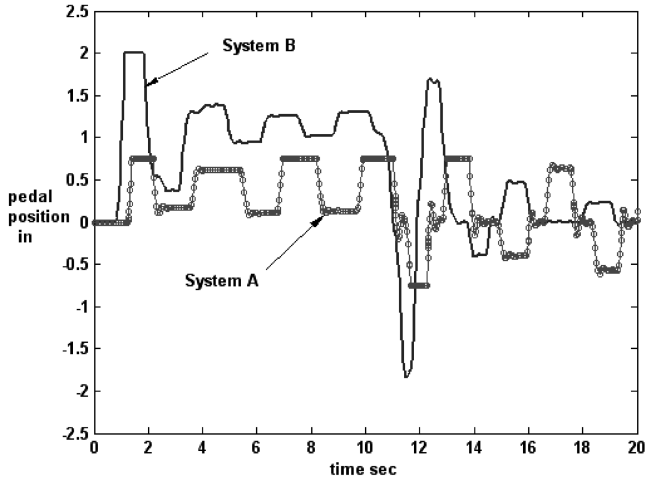

Fig. 10 Pedal position for systems A and B in wings-level sideslip capture task Note expanded abscissa scale as compared with Figs. 8 and 9.

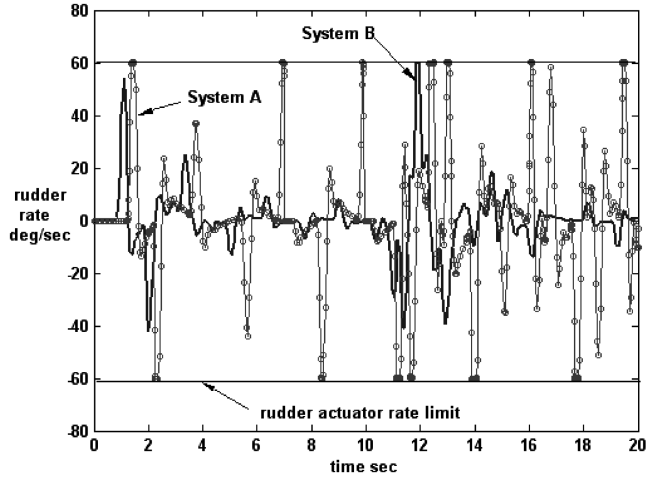

Fig. 11 Rudder rates for systems A and B in wings-level sideslip capture task; Note expanded abscissa scale as compared with Figs. 8 and 9.

D. Heading-Hold Sideslip-Capture Piloting Task

The possibility of employing a task slightly different than maintaining "wings level" with wheel inputs was next considered. This involved maintaining a desired heading with wheel inputs in the

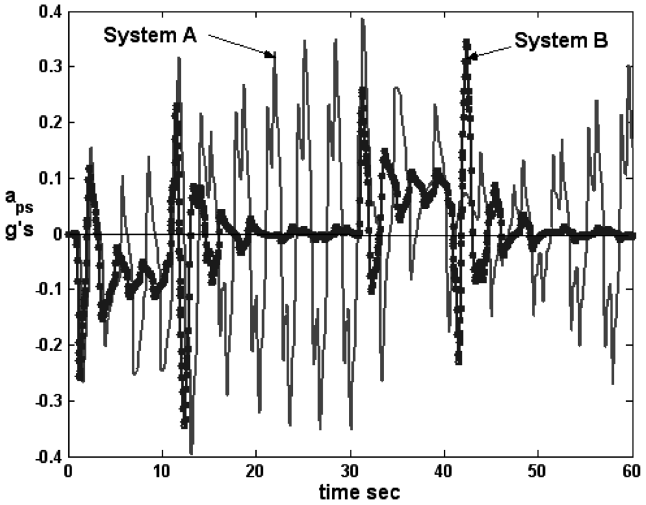

Fig. 12 Lateral acceleration at pilot's station for systems A and B in wings-level sideslip capture task.

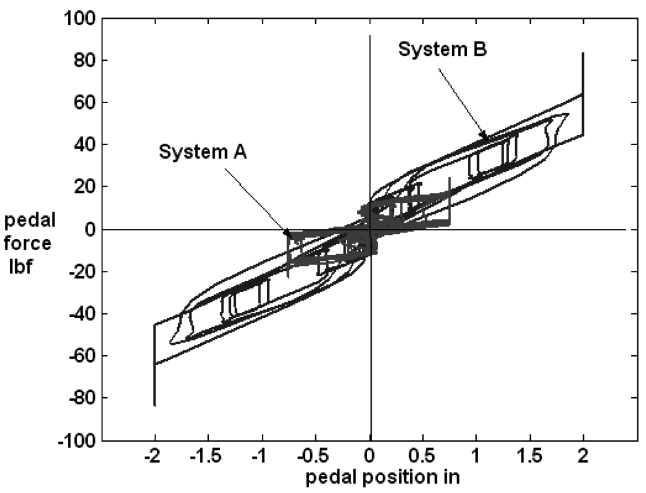

Fig. 13 Pedal force/feel systems—dynamic characteristics for wings-level sideslip capture task.

sideslip-capture task, here referred to as a "heading-hold sideslip-capture task." Fig. 14 shows the Bode plot of the transfer function

$$\left.\frac{\psi}{\phi_c}\right|_{\beta\to\delta_p;\phi\to\delta_w}$$

This represents the heading to roll command transfer function for the DC-8 aircraft with heading constrained by pedal inputs and roll constrained by wheel inputs. The constraints are created by the pilot models described previously. For this task, crossover frequencies for roll and sideslip loops were again 1 rad/s and 2 rad/s, respectively. Figure 14 indicates that in order to maintain adequate stability margins without the necessity of lead equalization on the part of the pilot in heading control, the heading loop can be closed with a crossover frequency no larger that approximately 0.4 rad/s. Table 2 shows the performance requirements for this task. As was the case in Table 1, the requirements have been chosen simply for the purposes of exposition.

Figures 15–20 show computer simulation results for this task that correspond to Figs. 8–13 for the wings-level sideslip-capture task. Once again, the lag apparent in Fig. 17 for system A is due to the larger hysteresis for that system. The responses indicate that system A from Fig. 3 does not meet the performance requirements of Table 2 (Fig. 15 shows system A violating the sideslip performance requirements). By comparison, system B does meet the requirements. A final comparison of Figs. 8–12 with Figs. 15–19 indicates

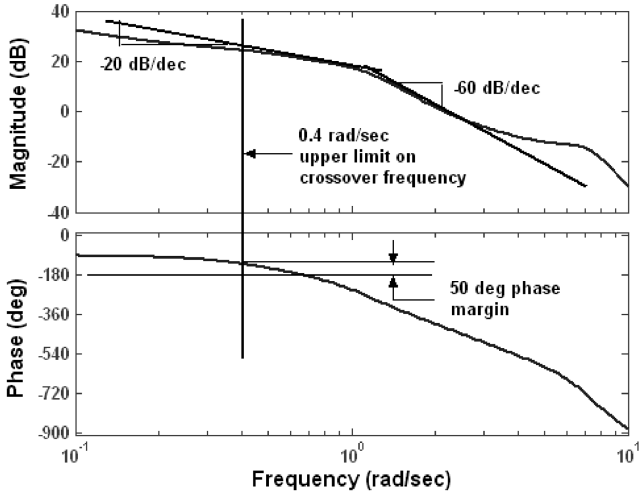

Fig. 14 Bode plot of $\frac{\psi}{\phi_c}|_{\beta\to\delta_p;\phi\to\delta_w}$ transfer function with pilot models in place.

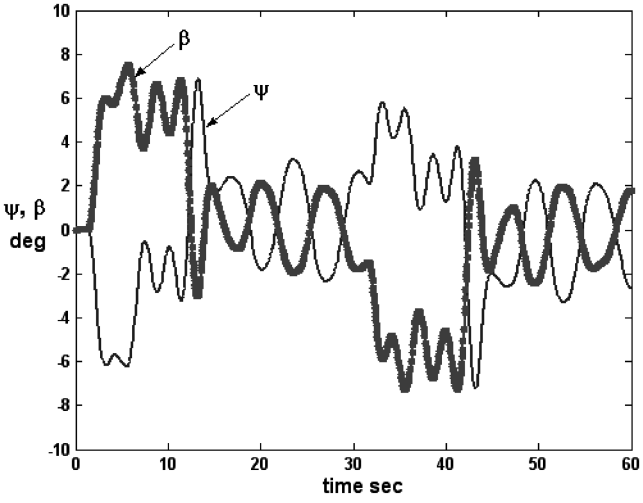

Fig. 15 Tracking performance using pedal force/feel system A from Fig. 3 in heading-hold sideslip-capture task.

that the wings-level sideslip-capture task may be more sensitive to rudder system characteristics than the heading-hold sideslip-capture task.

V. Force/Feel System Design Considerations

A. Human Pilot Pedal Force-Generation Capabilities

The force-generation capability of the human pilot is of definite interest in this study. A thorough study of muscular strength of both male and female subjects was reported in Meyer et al. [11]. Volunteer subjects included 458 male and 152 female naval aviation students and naval academy midshipmen. Muscle testing equipment was used to measure the strength and endurance of muscles in the arm, shoulder, and leg. The purpose of the report was to establish strength standards for aviation candidates for operating foot and hand controls. For strength assessment, the speed of movement was set to

Table 2 Performance requirements for heading-hold sideslip-capture task

Sideslip β	Heading ψ	Pedal inputs
Maximum steady-state error less than 0.5 deg No sustained oscillations greater than 1 deg	Maximum heading excursion ± 15 deg No sustained oscillations	No "stop-to-stop" reversals

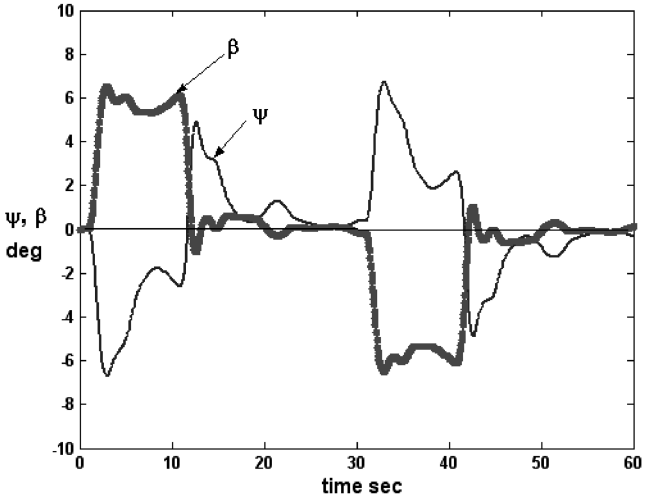

Fig. 16 Tracking performance using pedal force/feel system B from Fig. 3 in heading-hold sideslip capture task.

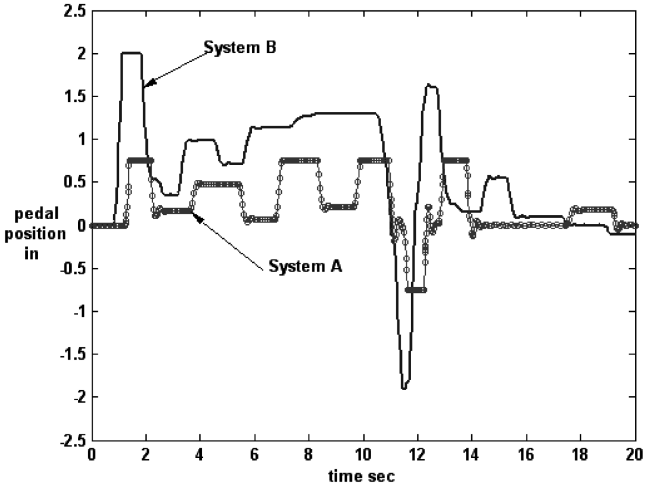

Fig. 17 Pedal position for systems A and B in heading-hold sideslip capture task. Note expanded abscissa scale as compared with Figs. 15 and 16.

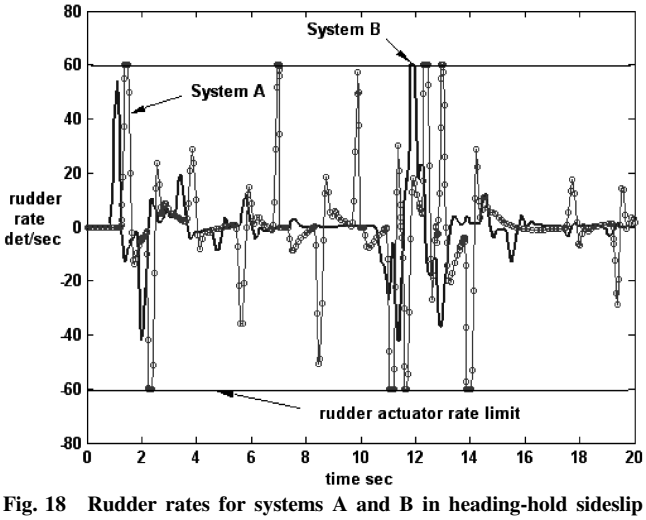

Fig. 18 Rudder rates for systems A and B in heading-hold sideslip capture task. Note expanded abscissa scale as compared with Figs. 15 and 16.

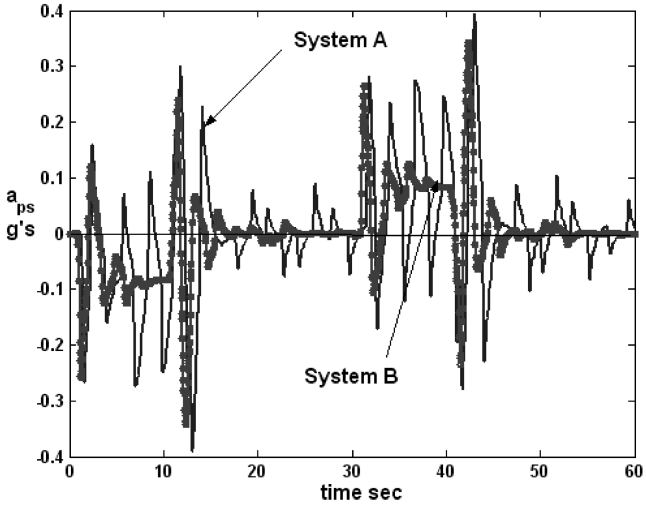

Fig. 19 Lateral acceleration at pilot's station for systems A and B in heading-hold sideslip capture task.

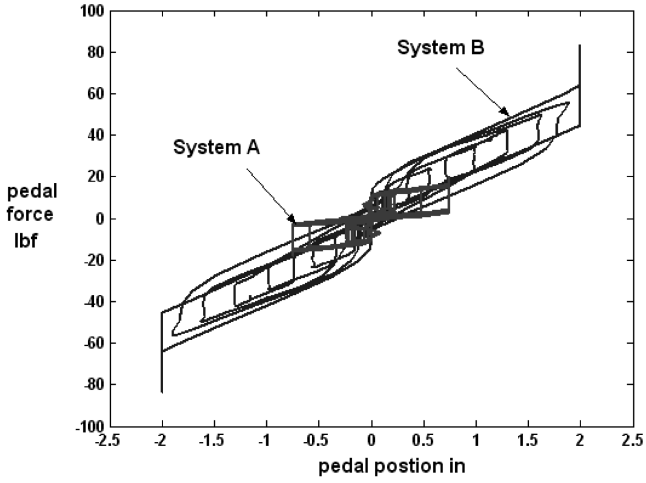

Fig. 20 Pedal force/feel systems: dynamic characteristics in heading-hold sideslip capture task.

60 deg/s and three to four maximal-exertion repetitions at 180 to 240 deg/s were done for endurance assessment on the same muscle group. Only the right side of the body was tested.

Three major muscle groups in the body were tested because of their involvement in performing critical occupational tasks in aviation: The large muscles of the upper leg that extend and flex the knee (quadriceps and hamstrings), the muscles acting on the shoulder joint to cause rotation, and the elbow extensors and flexors (biceps and triceps). Attention will be focused here upon the results for the leg and knee. Figure 21 summarizes the results for muscular strength and muscular endurance variables. As the figure indicates, there are significant differences between male and female subjects in both strength and endurance of the quadriceps and hamstrings. The female candidates exhibited only about 65% of the strength of their male counterparts. Similar comparisons of male and female strength can be found in Laubach [12]. This would perhaps suggest that maximum pedal forces required in any force/feel system be reduced from the 150 lbf recommended in FAR 25.143 subpart B c) to approximately 100 lbf for both male and female pilots. It should be noted that Woodson [13] recommends the 150 lbf limit based upon the capability of male subjects, alone.

B. Revised Linearity Index

The "linearity index" introduced in [6,7] and defined in Eq. (2) assumed that the "breakout" and "friction" forces were identical and that the friction force did not affect breakout. This means that the

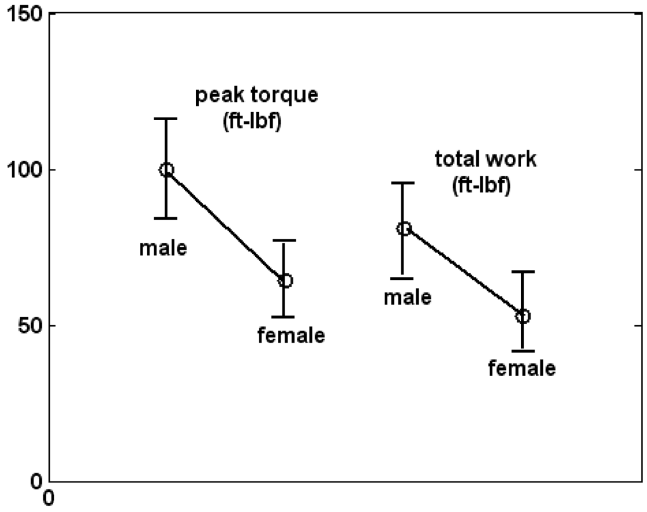

Fig. 21 Means and standard deviations of muscular strength and muscular endurance variables from Meyer et al. [11].

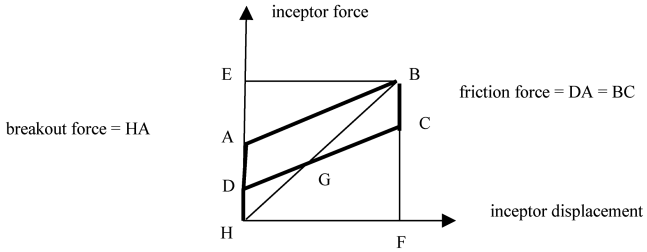

Fig. 22 Revised definition of a "linearity index."

force vs displacement graphs were parallelograms in the first and third quadrants. Figure 22 shows a more realistic representation. It is still assumed that friction does not affect breakout. Equation (4) defines a linearity index modified to account for these changes.

$$\mathrm{LI} = 1 - \frac{\text{area(HABH)} + \text{area(GBCG)}}{\text{area(HEBFH)}} \tag{4}$$

It is possible that the LI of Fig. 22 and Eq. (4) can be used as a design guide for force/feel systems. In this approach, a minimum acceptable value of the LI is identified along with desired breakout and friction forces. The following parameters are defined from Fig. 22.

F_{BO} = breakout force (HA in Fig. 22)
F_M = maximum force (HE in Fig. 22)
F_F = friction force (BC in Fig. 22)
δ_M = maximum displacement (HF in Fig. 22)
F_G = force gradient (slope of either line AB or DC in Fig. 22)

These parameters are not all independent. Including the constraint of a desired value of LI, the following relation can be derived from Fig. 22.

$$\mathrm{LI} = 1 - \frac{(F_{\mathrm{BO}}/2) + (F_F^2/2F_{\mathrm{BO}})}{F_{\mathrm{BO}} + F_G\delta_M} \tag{5}$$

The remaining constraint for using Eq. (6) is that is that the slopes of lines AB and DC are identical. The selection of F_{BO} can be guided by operational considerations. For example, minimum values of F_{BO} and F_F could be based upon a desire to minimize unintentional inputs caused by cockpit accelerations or pilot changes in seating posture. Now assume that it is desired to obtain LI = 0.8, with $F_{\mathrm{BO}} = 10$ lbf and $F_F = 10$ lbf. Equation (5) will yield

$$F_G\delta_M = 40 \text{ lbf} \tag{6}$$

a value well below the 100 lbf suggested in part A of this section. The designer can now choose a force gradient F_G. The selection of this

gradient will determine the lateral acceleration in g's at the pilots' station per pound of pedal force above breakout at each flight condition. As will be seen in Sec. V.C, a maximum value of this ratio is recommended. This maximum value would then yield a desired minimum value of F_G. If, for example, the resulting minimum $F_G = 15$ lbf/in, then $\delta_M = 2.67$ inches.

C. The "Virtual" Bobweight and Pedal Force per G of Yaw Acceleration

Bobweights have long been used to alter the effective longitudinal response characteristics of aircraft to column or longitudinal control inceptor inputs [14]. The first effect of such devices is an increase in the stick force per g. In this light, bobweights act as a safety feature, providing proprioceptive feedback information to the pilot as regards normal accelerations caused by control inputs. In addition, they provide a constant stick-force per g across the flight envelope. The dynamic effect of bobweights is more complicated, as it alters system transfer functions such as $(n_{cg_z}/\delta_F)(s)$ where n_{cg_z} is the normal acceleration at the aircraft center of gravity and δ_F is the longitudinal force applied to the control inceptor (column or stick). It is interesting at this juncture to consider a brief survey of the effect of a bobweight on rudder control. Consider Fig. 23 which is a schematic representation of a rudder bobweight. Note that the positive yaw acceleration shown will create an "inertial" moment about the pedal axis in the direction shown. Effectively, this would mean that the pilot would have to apply a larger force to the right pedal to maintain the current desired pedal input. The inertial moment is an obvious function of the bobweight mass and its distance from both the rudder pedal axis of rotation and the aircraft center of gravity. In Fig. 23, this moment is shown as $K_{BW} \cdot \dot{r}$, where K_{BW} subsumes the mass and geometry parameters just mentioned. Figure 24 shows the Bode plots of the transfer function $(\dot{r}/\delta_{PF})(s)$ (yaw acceleration to pedal force input) for the DC-8 aircraft used in this study for two values of K_{BW}. Mass and geometry parameter values are simply chosen here to demonstrate the effect of a virtual bobweight on this transfer function. The rudder actuator dynamics of Eq. (1) and the pedal force/feel dynamics of Eq. (3) are included, but not the yaw damper. The term virtual is used here to emphasize the fact that the bobweight effect could be created artificially in the pedal force/feel system. This is particularly true if a fly-by-wire rudder control system is being used. The effect of K_{BW} is seen to reduce the magnitude of the $(\dot{r}/\delta_{PF})(s)$ transfer function over a broad frequency range from 0.1 to over 20 rad/s. The 4.3 dB reduction is equivalent to a 64% increase in the pedal force per unit of yaw acceleration in the rudder pedals. It should be noted that any further increase in K_{BW} here will result in a destabilization of the high-frequency mode around 20 rad/s (emanating from the roots of the force/feel system dynamics).

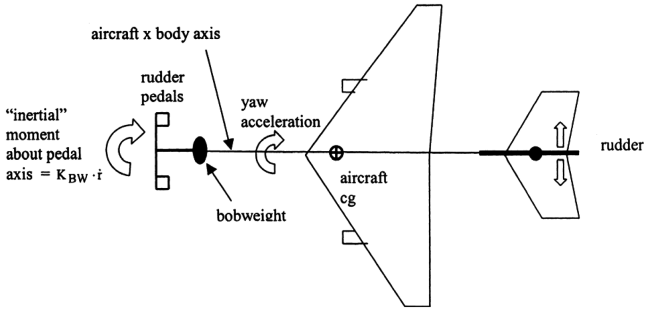

Fig. 23 A rudder "bobweight."

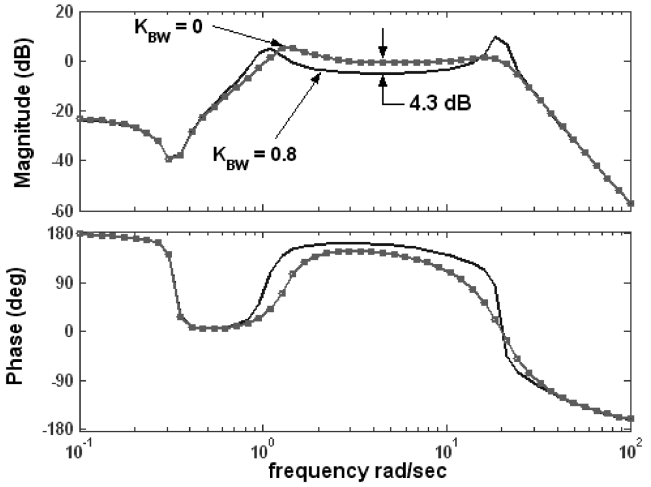

Fig. 24 Bode plots of $(\dot{r}/\delta_{PF})(s)$ transfer function showing virtual bobweight effect.

It is reasonable to propose at this juncture that the magnitude of the $(\dot{r}/\delta_{PF})(s)$ transfer function may be a harbinger of the excessively large aircraft motion (acceleration) that can create the handling qualities cliffs alluded to in Sec. IV.C. This is particularly true if large magnitudes of $(\dot{r}/\delta_{PF})(s)$ occur in combination with pedal force/feel systems with small values of the linearity index.

This brief analysis suggests that the number of g's of lateral acceleration at the pilot's station per pound of pedal force beyond breakout may be an important certification factor. Yaw acceleration in rad/s^2 may be substituted for lateral acceleration at the pilot's station. As a point of reference, for the example DC-8 aircraft at the flight condition chosen, the number of g's of lateral acceleration at the pilot's station per pound of pedal force is approximately 0.022 for system A and 3.5×10^{-3} for system B. This yields a ratio of 6.3 between the two.

An initial estimate for maximum value of the lateral acceleration at the pilot's station per pound of pedal force might be 5×10^{-3} g per pound. The value 5×10^{-3} g per pound is little more than a reasonable guess at this point, and the maximum value would typically be evaluated at flight conditions involving maximum dynamic pressure. Some limited data is available to support the value quoted, however. Hoh et al. [15] describes flight test results in which the Princeton Navion variable response aircraft (VRA) was configured to investigate wings-level turn modes. The data pertinent to this discussion are very limited. Figures 25 and 26 demonstrate a sharp degradation in handling qualities ratings when the lateral g's per pound of pedal force increase beyond 0.005. In Fig. 25, "favorable yaw coupling" refers to the *tendency* of the nose of the aircraft to move in the direction of commanded turn, while in Fig. 26, "favorable roll coupling" refers to the *tendency* of the aircraft to roll in the direction of the commanded wings-level turn. The different symbols in Figs. 25 and 26 represent the Cooper–Harper ratings assigned by different pilots. Three facts must obviously be borne in mind in considering these results. First, the data is sparse. Second, the vehicle is not a transport aircraft. Third, the command/response characteristics for pedal inputs (wings-level turn) are not representative of those of a transport aircraft. Nonetheless, the sharp degradation in handling qualities that did occur for the lateral g's per pound of pedal force beyond 0.005 suggests that this value may be worthy of further scrutiny as a limit for maximum pedal sensitivity.

D. Dynamic Force/Feel System Considerations

Figures 5 and 6 clearly show that the static force/feel system characteristics are altered when dynamic effects are considered. This is due to the finite bandwidth of the force/feel system dynamics. In addition, the linear and nonlinear effects of surface actuators affect the relationship between applied inceptor force and control surface movement. A linearity index that encompasses these dynamic effects can be defined in addition to that for quasistatic displacements focusing on the force/feel system, alone. Obviously, a small linearity index value for quasistatic deflections will not increase in magnitude (improve) when dynamics effects are considered. Determining both index values, however, will help uncover just where limitations in linearity arise in the force/feel-actuator system. Figure 27 demonstrates *overall* linearity characteristics for the vehicle analyzed here with force/feel system B (see Fig. 3). In this figure, a sinusoidal pedal force is being applied at the frequency of the

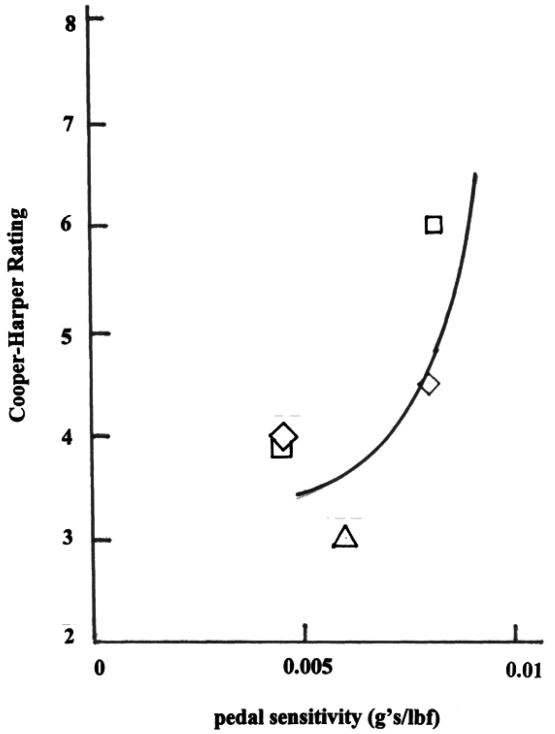

Fig. 25 Pedal sensitivity data from Hoh et al. [15] (high favorable yaw coupling); different symbols indicate different evaluation pilots.

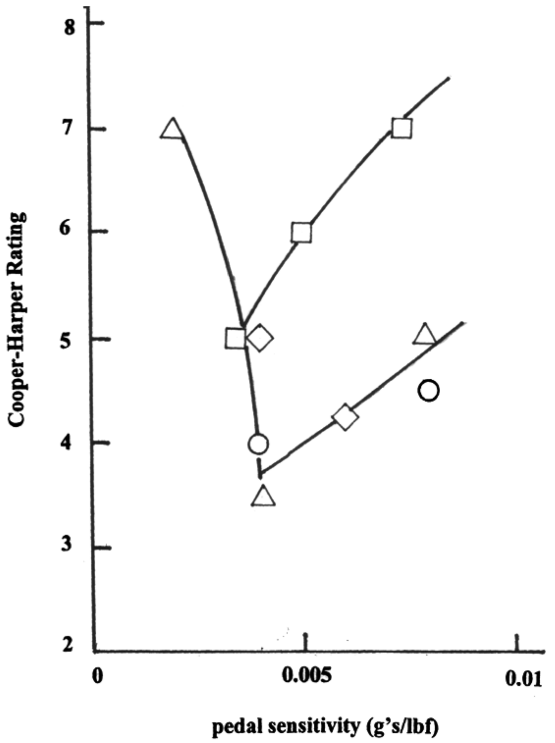

Fig. 26 Pedal sensitivity data from Hoh et al. [15] (very high favorable roll coupling); different symbols indicate different evaluation pilots.

aircraft's dutch roll mode, and with an amplitude approximately creating the maximum pedal displacement. Using the dutch roll frequency for creating Fig. 27 can be justified by referring to Fig. 24. There one sees the relatively flat section of the magnitude plot beginning at around 1 rad/s which is the approximate location of the dutch roll natural frequency for this vehicle and flight condition. In Fig. 27, the rudder actuator rate limit was reduced by 50% to demonstrate the effect of this limitation on overall linearity. Note that

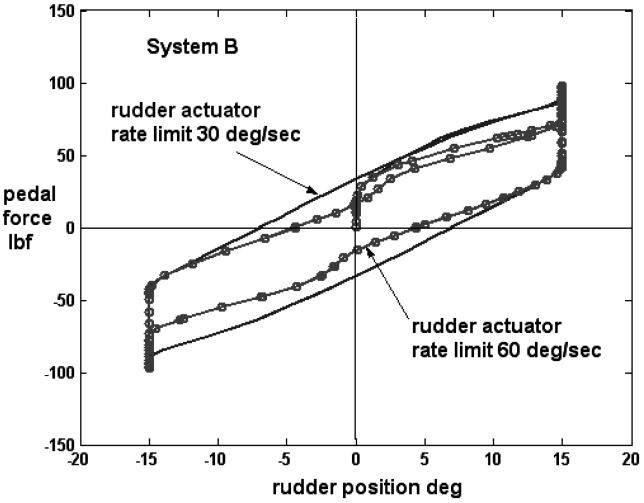

Fig. 27 Effect of force/feel system dynamics and rudder actuator characteristics on pedal force vs rudder position for force/feel system B.

Performance – Hovering Turn

	Scout/Attack		Cargo/Utility	
	GVE	DVE	GVE	DVE
DESIRED PERFORMANCE				
• Maintain the longitudinal and lateral position within ±X ft of a point on the ground	3 ft	6 ft	3 ft	6 ft
• Maintain altitude within ±X ft:	3 ft	3 ft	3 ft	3 ft
• Stabilize the final rotorcraft heading at 180 deg from the initial heading within ±X deg:	3 deg	5 deg	5 deg	5 deg
• Complete turn to a stabilized hover (within the desired window) within X seconds from initiation of the maneuver	10 sec	15 sec	15 sec	15 sec
ADEQUATE PERFORMANCE				
• Maintain the longitudinal and lateral position within ±X ft of a point on the ground	6 ft	12 ft	6 ft	12 ft
• Maintain altitude within ±X ft:	6 ft	6 ft	6 ft	6 ft
• Stabilize the final rotorcraft heading at180 deg from the initial heading within ±X deg:	6 deg	10 deg	10 deg	10 deg
• Complete turn to a stabilized hover (within the desired window) within X seconds from initiation of the maneuver	15 sec	15 sec	20 sec	20 sec

Fig. 28 A rotorcraft task description from [16].

a linearity index defined using this figure would decrease from that of the quasistatic force/feel system alone when the effects of force/feel and actuator dynamics are included. It is suggested that the linearity index be calculated using the variables shown in Fig. 27, that is, rudder displacement and pedal force, and with a pedal input representing maximum displacements using a sinusoidal force at a frequency approximating the dutch roll mode frequency at a variety of flight conditions. A minimum value of this overall linearity index of 0.6 might be suggested.

VI. Force/Feel System Comparison

Some light may be shed on the desirable characteristics of rudder pedal force/feel systems by examining and cataloging the pedal force/feel systems in aircraft that require precise yaw control as a typical part of their operational tasks. For example, the handling qualities of modern military rotorcraft are ascertained through the completion of well-defined low-speed flight tasks in which specific performance requirements are called out [16]. Figure 28 is taken from [16] and describes one such task, the "hover turn." Note that precise heading control is required of the pilot/vehicle system. In this light, a comparison of the static pedal force/feel system characteristics of representative military rotorcraft may be warranted. Four such rotorcraft were chosen for study. These included an attack helicopter (AH), a utility helicopter (UH), a tandem rotor cargo helicopter (CH1) and a large, single-rotor cargo helicopter (CH2). If an examination of the linearity indices for these vehicles indicates that relatively small values were in evidence, for example, LI < 0.5, then serious doubt would be cast upon the

Table 3 Linearity indices for selected aircraft pedal force/feel systems

Vehicle	Linearity index
TA3	0.4
AH	0.6
UH	0.62
CH2	0.64
TA2	0.81
CH1	0.82
TA1	0.86

supposition that this index can be useful in discriminating between good and poor force/feel designs.

In the comparison to be undertaken, the linearity indices of three transport aircraft were also included. These aircraft are denoted TA1, TA2, and TA3 (with the latter at 240 kts airspeed). Each of these vehicles is of comparable size. Indeed TA2 is the immediate predecessor of TA3 and is from the same manufacturer. A particular airspeed was called out for TA3 because the characteristics of the rudder force/feel system changes with airspeed for this vehicle. This is not true for any of the remaining vehicles, including the rotorcraft. Table 3 shows the values of the linearity indices for the six aircraft just described ranked in order of increasing LI value. These indices were calculated using Eq. (4) and straight-line approximations to the vehicle pedal force/feel systems. Note that the rotorcraft have LI values ranging from 0.6 to 0.82. These relatively large values provide some support for the utility of the linearity index.

VII. Discussion

The study summarized in the preceding sections was aimed at identifying candidate methodologies for certification of rudder force/feel systems that would reflect the philosophy of AC 25-7A [2]. The analytical treatment was preceded by an overview of current FAA certification standards to place the research in context. The study suggests that rudder force/feel systems that exhibit small linearity index values or are characterized by large lateral accelerations per pound of pedal force beyond breakout can be potentially hazardous, especially if used in high-gain tracking tasks by the pilot. The study has deliberately avoided asking whether such high-gain tracking is appropriate in different flight tasks, only attempting to estimate when might happen if such behavior indeed occurs.

As initial estimates, one could require a minimum value of the quasistatic force/feel linearity index of 0.7, a minimum value of the overall linearity index of 0.6. In addition, a maximum value for the force required for maximum pedal deflection of 100 lbf may be suggested based upon comparative anthropometric studies of male and female subjects. Finally, a maximum value of the cockpit lateral acceleration per pound of applied pedal force might be specified. This actual value of this ratio would be determined by applying sinusoidal pedal inputs at the aircraft's dutch roll frequency at points in the flight envelope of maximum dynamic pressure is in evidence. A maximum value of 0.005 g's per pound of pedal force above breakout might provide an initial estimate. Of course, further refinement of all of these criterion values is necessary. If appropriate criterion values for the linearity indices and lateral acceleration can be found, these metrics could serve as a means for reviewing the designs of existing transport aircraft. Future certification standards could include evidence that all these metrics meet criterion values.

Piloted simulation of the wings-level sideslip-capture task could be suggested as a means for manufacturers to assess the rudder force/feel systems for future aircraft, in the spirit of AC-25-7A. Special sensor/display requirements and flight safety issues would probably eliminate this task as part of a certification effort. In terms of display requirements for conducting the task in piloted simulation, a head-up display can be employed with the only requirement being the display of the aircraft velocity vector and artificial horizon. Simulation is suggested because the nature of the proposed task carries an obvious risk for flight test. To this end it is worth recalling a statement for AC 25-7A: *However, for conditions that are considered too dangerous to attempt in actual flight . . . the closed-loop evaluation tasks may be performed using a motion-base high-fidelity simulator if it can be validated for the flight conditions of interest*.

In closing it should be emphasized that the certification and design issues addressed in this report are not proposed as a methodology to optimize handling qualities vis-à-vis the rudder control system. Rather they are offered as a means of establishing minimum characteristics for safe flight.

VIII. Conclusions

Based upon the preliminary research summarized herein, the following conclusions can be drawn.

1) Current certification requirements for rudder force/feel systems may not be sufficient to identify potentially dangerous designs.

2) A candidate task for evaluating rudder force/feel systems can be suggested following the general philosophy of FAA advisory circular 25-7A, namely a wings-level sideslip-capture task. Because special sensors/displays may be required for this task (sideslip sensing and display) it would not be suitable for a certification task. In addition, potential flight safety issues would probably limit its use to high-fidelity motion-base simulators.

3) A competing lateral-directional control task, namely a heading-hold sideslip-capture task was found analytically to be less sensitive to variations in rudder control system characteristics than the wings-level sideslip-capture task.

4) Based upon anthropometric studies of both male and female subjects, it may be advisable to limit maximum rudder pedal forces to 100 lbf in transport aircraft.

5) A linearity index can be defined that provides a simple measure of force/feel system linearity and linearity of the overall rudder control system. Small values of this index indicate highly nonlinear control characteristics.

6) The yaw acceleration (or lateral acceleration at the pilot's station) per pound of pedal force above breakout is an important sensitivity parameter in rudder and force/feel system design. Large values of this ratio indicate a sensitive rudder system.

7) The following may warrant further investigation for certification standards: a) a minimum value of the linearity index when pedal force is plotted vs *pedal deflection* in quasistatic fashion (initial estimate 0.7). b) a minimum value of the linearity index when pedal force is plotted vs *rudder deflection* with a sinusoidal applied force yielding the maximum pedal deflection at the largest dutch roll natural frequency in evidence across the flight envelope (initial estimate 0.6). c) a maximum value of g's of lateral acceleration at the cockpit per pound of pedal force above breakout evaluated at flight condition of maximum dynamic pressure (initial estimate 5×10^{-3} g's per pound). d) a maximum value of required pedal force (initial estimate 100 lbf).

Acknowledgements

The research reported herein was supported by a grant from the Federal Aviation Administration, through the William J. Hughes Technical Center, Atlantic City International Airport, NJ. The grant technical manager is Robert McGuire. The conclusions drawn in this study are those of the author and do not necessarily reflect those of the Federal Aviation Administration.

References

[1] Anon., "In-Flight Separation of Vertical Stabilizer American Airlines Flight 587 Airbus Industrie A300-605R, N14053, Belle-Harbour, New York, Nov., 12, 2001," National Transportation Safety Board, Accident Report No. NTSB/AAR-04/04, Oct. 2004.

[2] Anon., *Advisory Circular 25-7A: Flight Test Guide for Certification of Transport Category Airplanes*, U.S. Department of Transportation, Federal Aviation Administration, Washington, DC, 31 March, 1998.

[3] Thiel, G. C., "FAA's History with APC," *Pilot-Induced Oscillation Research: Status at the End of the Century*, CP-2001-210389, Vol. 1, NASA, Washington, DC, April 2001, pp. 95–105.

[4] Lee, B. P., "PIO Flight Test Experience at Boeing (Puget Sound)," *Pilot-Induced Oscillation Research: Status at the End of the Century*,

Vol. 1, NASA, Washington, DC, April 2001, pp. 109–155.
[5] Poncelet, P., and Alonso, F., "Flight Testing for APC; Current Practice at Airbus," *Pilot-Induced Oscillation Research: Status at the End of the Century*, CP-2001-210389, Vol. 1, NASA, Washington, DC, April 2001, pp. 179–180.
[6] Hess, R. A., "Handling Qualities and Flight Safety Implications of Rudder Control Strategies and Systems in Transport Aircraft," U.S. Department of Transportation, Federal Aviation Administration, Rept. DOT/FAA/AR-05/212, June 2005.
[7] Hess, R. A., "Rudder Control Strategies and Force/Feel System Designs in Transport Aircraft," *Journal of Guidance, Control, and Dynamics*, Vol. 28, No. 6, 2005, pp. 1251–1262.
[8] McRuer, D., Ashkenas, I., and Graham, D., *Aircraft Dynamics and Automatic Control*, Princeton University Press, Princeton, NJ, 1973, Chap. 8.
[9] Hess, R. A., "Feedback Control Models—Manual Control and Tracking," in *Handbook of Human Factors and Ergonomics*, edited by G. Salvendy, Wiley, New York, 1997, Chap. 38.
[10] Anon., *Aviation Safety and Pilot Control, Understanding and Preventing Unfavorable Pilot-Vehicle Interactions*, National Academy Press, Washington, DC, 1997, Chap. 2.
[11] Meyer, L. G., Pokorski, T. L, Ortel, B. E., Saxton, J. L., and Collyer, P. D., "Muscular Strength and Anthropometric Characteristics of Male and Female Naval Aviation Candidates," Naval Aerospace Medical Research Laboratory, Rept. NAMRL-1396, Pensacola, FL, Dec. 1996.
[12] Laubach, L. L., "Human Muscular Strength," NASA RP 1024, July 1978.
[13] Woodson, W. E., *Human Factors Design Handbook*, McGraw–Hill, New York, 1981, Chap. 4.
[14] McRuer, D. T., and Johnston, D. E., "Flight Control Systems Properties and Problems," NASA CR-2500, Feb. 1975.
[15] Hoh, R. H., Myers, T. T., Ashkenas, I. L., Ringland, R. F., and Craig, S. J., "Development of Handling Quality Criteria for Aircraft with Independent Control of Six Degrees of Freedom," Air Force Wright Aeronautical Laboratories, Rept. AFWAL-TR-81-3027, Wright–Patterson AFB, OH, April 1981.
[16] Anon., "Aeronautical Design Standard, Performance Specification, Handling Qualities Requirements for Military Rotorcraft," U.S. Army Aviation and Missile Command, Rept. ADS-33E-PRF, Redstone Arsenal, AL, March 2000.